

A modular A_4 symmetric scotogenic model

Takaaki Nomura,^{1,*} Hiroshi Okada,^{2,3,†} and Oleg Popov^{4,‡}

¹*School of Physics, KIAS, Seoul 02455, Republic of Korea*

²*Asia Pacific Center for Theoretical Physics (APCTP) - Headquarters San 31,
Hyoja-dong, Nam-gu, Pohang 790-784, Korea*

³*Department of Physics, Pohang University of Science
and Technology, Pohang 37673, Republic of Korea*

⁴*Institute of Convergence Fundamental Studies,
Seoul National University of Science and Technology,
Seoul 139-743, Korea*

(Dated: March 16, 2020)

Abstract

We propose a minimal extension of the Standard Model where neutrino masses are generated radiatively at one-loop level via Scotogenic scenario. The model is augmented with A_4 modular symmetry as a scotogenic and flavor symmetry. With minimal number of parameters, the model makes predictions for neutrino oscillation data, Majorana and Dirac phases, dark matter characteristics, and neutrinoless double beta decay.

*Electronic address: nomura@kias.re.kr

†Electronic address: hiroshi.okada@apctp.org

‡Electronic address: opopo001@ucr.edu

I. INTRODUCTION

Particle physics experiments and observations have been successfully confirming the standard model (SM) of particle physics. On the other hand, there are some issues indicating an existence of physics beyond the SM such as existence of dark matter (DM), non-zero tiny neutrino masses and origin of flavor structure. In describing these issues, symmetry would play an important role like guaranteeing stability of DM, forbidding neutrino mass at tree level and restricting flavor structure. It is thus interesting to construct a model of physics beyond the SM adopting a new symmetry.

Modular flavor symmetries have been recently proposed by [1, 2] to provide more predictions to the quark and lepton sector due to Yukawa couplings with a representation of a group. Their typical groups are found in basis of the A_4 modular group [2–11], S_3 [12–15], S_4 [16–18], A_5 [19, 20], larger groups [21], multiple modular symmetries [22], and double covering of A_4 [23] in which masses, mixings, and CP phases for quark and lepton are predicted.¹ Also, a systematic approach to understand the origin of CP transformations has been recently achieved by ref. [32]. In particular a model with modular A_4 symmetry is discussed in ref. [6, 11] where neutrino mass is generated at one-loop level. For model in ref. [6], inert doublet and singlet scalar fields are introduced to generate neutrino mass using modular form of weight 2 which is a triplet of A_4 and the basis for constructing other modular forms with higher weight. On the other hand, for model in ref. [11], vector-like leptons are introduced to get positive contribution to muon $g - 2$ and triplet modular form with weight 4 is used.

In this paper, we apply modular A_4 symmetry in minimal Scotogenic model [33] in which neutrino mass is generated at one-loop level and DM candidates are contained. We find that the minimal Scotogenic model can be realized by use of modular forms with higher weight which are constructed by that of weight 2. Thus field contents and the structure of model are much simpler than previous models [6, 11]. In our construction the right-handed neutrinos are introduced as a triplet of A_4 assigning modular weight $-k = -1$. Also, non-zero modular weight is assigned to inert Higgs doublet as $-k = -3$. Interestingly we find that additional Z_2 symmetry is not necessary to realize structure of Scotogenic model due

¹ Several reviews are helpful to understand the whole idea [24–31].

	Fermions			Bosons	
	$(\bar{L}_{L_e}, \bar{L}_{L_\mu}, \bar{L}_{L_\tau})$	$(e_{R_e}, e_{R_\mu}, e_{R_\tau})$	N_R	H	η^*
$SU(2)_L$	2	1	1	2	2
$U(1)_Y$	$\frac{1}{2}$	-1	0	$\frac{1}{2}$	$-\frac{1}{2}$
A_4	$1, 1', 1''$	$1, 1'', 1'$	3	1	1
$-k$	0	0	-1	0	-3

TABLE I: Fermionic and bosonic field content of the model and their charge assignments under $SU(2)_L \times U(1)_Y \times A_4$ in the lepton and boson sector, where $-k$ is the number of modular weight and the quark sector is the same as the SM.

	Couplings		
	$Y_1^{(6)}$	$Y_3^{(2)}$	$Y_3^{(4)}$
A_4	1	3	3
$-k$	6	2	4

TABLE II: Modular weight assignments for Yukawas.

to the nature of modular form. Then numerical analysis for neutrino mass matrix is carried out to show predictions of our model as a result of modular A_4 symmetry.

Manuscript is organized as follows. In Sec. II, we give our model set up under A_4 modular symmetry. We discuss right-handed neutrino mass spectrum, lepton flavor violation (LFV) and generation of the active neutrino mass at one-loop level in Sec. III. Numerical analysis is presented in Sec. IV. Finally, we conclude and discuss in Sec. V.

II. MODEL

In this section we introduce our model, which is based on A_4 modular symmetry. Leptonic and scalar fields of the model and their representations under A_4 symmetry and modular weights are given by Tab. I, while the ones of Yukawa couplings are given by Tab. II.

Under these symmetries, we write renormalizable Lagrangian as follows:

$$\begin{aligned}
-\mathcal{L}_{Lepton} &= \sum_{\ell=e,\mu,\tau} y_{\ell} \bar{L}_{L_{\ell}} H e_{R_{\ell}} \\
&+ \alpha_{\nu} \bar{L}_{L_e} (Y_{\mathbf{3}}^{(4)} \otimes N_R)_{\mathbf{1}} \tilde{\eta} + \beta_{\nu} \bar{L}_{L_{\mu}} (Y_{\mathbf{3}}^{(4)} \otimes N_R)_{\mathbf{1}'} \tilde{\eta} + \gamma_{\nu} \bar{L}_{L_{\tau}} (Y_{\mathbf{3}}^{(4)} \otimes N_R)_{\mathbf{1}'} \tilde{\eta} \\
&+ M_1 (Y_{\mathbf{3}}^{(2)} \otimes \bar{N}_R^C \otimes N_R) + \text{h.c.}, \tag{II.1}
\end{aligned}$$

where $\tilde{\eta} \equiv i\sigma_2 \eta^*$, σ_2 being second Pauli matrix, and charged-lepton matrix is diagonal thanks to the unique representation of A_4 .

The full symmetry of the leptonic sector of the model is $SU(2)_L \times U(1)_Y \times A_4$, where the \mathbb{Z}_2 symmetry of [33] is replaced with modular symmetry $\Gamma_3 \simeq A_4$. A_4 serves three purposes: flavor symmetry, scotogenic symmetry, and dark matter stabilizing symmetry.

The basis of modular form is the one with weight 2, $Y_{\mathbf{3}}^{(2)} = (y_1, y_2, y_3)$, transforming as a triplet of A_4 whose components are written in terms of Dedekind eta-function $\eta(\tau)$ and its derivative $\eta'(\tau)$ [2]:

$$\begin{aligned}
y_1(\tau) &= \frac{i}{2\pi} \left(\frac{\eta'(\tau/3)}{\eta(\tau/3)} + \frac{\eta'((\tau+1)/3)}{\eta((\tau+1)/3)} + \frac{\eta'((\tau+2)/3)}{\eta((\tau+2)/3)} - \frac{27\eta'(3\tau)}{\eta(3\tau)} \right), \\
y_2(\tau) &= \frac{-i}{\pi} \left(\frac{\eta'(\tau/3)}{\eta(\tau/3)} + \omega^2 \frac{\eta'((\tau+1)/3)}{\eta((\tau+1)/3)} + \omega \frac{\eta'((\tau+2)/3)}{\eta((\tau+2)/3)} \right), \\
y_3(\tau) &= \frac{-i}{\pi} \left(\frac{\eta'(\tau/3)}{\eta(\tau/3)} + \omega \frac{\eta'((\tau+1)/3)}{\eta((\tau+1)/3)} + \omega^2 \frac{\eta'((\tau+2)/3)}{\eta((\tau+2)/3)} \right). \tag{II.2}
\end{aligned}$$

Here the overall coefficient in Eq. (II.2) is one possible choice; it cannot be uniquely determined. Then, any modular forms of higher weight are constructed by the products of $Y_{\mathbf{3}}^{(2)}$ using multiplication rules of A_4 representations, and one finds the following higher weight modular forms:

$$Y_{\mathbf{1}}^{(6)} = y_1^3 + y_2^3 + y_3^3 - 3y_1 y_2 y_3, \quad Y_{\mathbf{3}}^{(4)} = \begin{bmatrix} y_1^2 - y_2 y_3 \\ y_3^2 - y_1 y_2 \\ y_2^2 - y_1 y_3 \end{bmatrix}. \tag{II.3}$$

Higgs potential of our model is equivalent to the potential of the Scotogenic model [33] without loss of generality, where a quartic coupling that plays the role in generating the nonzero neutrino masses is given by $Y_{\mathbf{1}}^{(6)} (H^\dagger \eta)^2$ term. The $(H^\dagger \eta)$ term that was forbidden in the inert two Higgs doublet model (2HDM) by \mathbb{Z}_2 invariance is now forbidden by modular invariance via A_4 . This is due to the fact that modular form with odd number of modular

weight does not exist; here the oddness of modular weight play a role of odd parity under Z_2 symmetry as shown in ref. [6].

The right-handed neutrino mass matrix is given by

$$M_N = \frac{M_1}{3} \begin{bmatrix} 2y_1 & -y_3 & -y_2 \\ -y_3 & 2y_2 & -y_1 \\ -y_2 & -y_{3,1} & 2y_3 \end{bmatrix}. \quad (\text{II.4})$$

Then, the Majorana mass matrix is diagonalized by an unitary matrix as $D_N \equiv UM_NU^T$, and their mass eigenstates are defined by ψ_R , where $N_R = U^T\psi_R$.

The Dirac Yukawa matrix is given by

$$y_\eta = \begin{bmatrix} \alpha_\nu & 0 & 0 \\ 0 & \beta_\nu & 0 \\ 0 & 0 & \gamma_\nu \end{bmatrix} \begin{bmatrix} y'_1 & y'_3 & y'_2 \\ y'_3 & y'_2 & y'_1 \\ y'_2 & y'_1 & y'_3 \end{bmatrix}, \quad (\text{II.5})$$

where $Y_{\mathbf{3}}^{(4)} \equiv (y'_1, y'_2, y'_3)$, and we impose the perturbative limit $\text{Max}[y_\eta] \lesssim \sqrt{4\pi}$ in the numerical analysis.

III. ANALYSIS

In this section we analyze lepton flavor violation and neutrino mass formulating analytic forms of branching ratio (BR) of $\ell_i \rightarrow \ell_j \gamma$ process and neutrino mass matrix.

Charged lepton flavor violating (cLFV) processes arise from Yukawa interactions associated with y_η coupling as in [38]. Considering the mixing matrix of N_R , we obtain the BRs such that

$$\text{BR}(\ell_i \rightarrow \ell_j \gamma) \approx \frac{48\pi^3 \alpha_{em} C_{ij}}{G_F^2 (4\pi)^4} \left| \sum_{\alpha=1-3} Y_{\eta j \alpha} Y_{\eta \alpha i}^\dagger F(D_{N_\alpha}, m_{\eta^\pm}) \right|^2, \quad (\text{III.1})$$

$$F(m_a, m_b) \approx \frac{2m_a^6 + 3m_a^4 m_b^2 - 6m_a^2 m_b^4 + m_b^6 + 12m_a^4 m_b^2 \ln\left(\frac{m_b}{m_a}\right)}{12(m_a^2 - m_b^2)^4}, \quad (\text{III.2})$$

where $Y_\eta \equiv y_\eta U^T$, $C_{21} = 1$, $C_{31} = 0.1784$, $C_{32} = 0.1736$, $\alpha_{em}(m_Z) = 1/128.9$, and $G_F = 1.166 \times 10^{-5} \text{ GeV}^{-2}$. The experimental upper bounds are given by [39–41]

$$\text{BR}(\mu \rightarrow e \gamma) \lesssim 4.2 \times 10^{-13}, \quad \text{BR}(\tau \rightarrow e \gamma) \lesssim 3.3 \times 10^{-8}, \quad \text{BR}(\tau \rightarrow \mu \gamma) \lesssim 4.4 \times 10^{-8}, \quad (\text{III.3})$$

which will be imposed in our numerical calculation as constraints.

Neutrino mass matrix at one-loop level can be derived as

$$m_{\nu_{ij}} \approx \sum_{\alpha=1-3} \frac{Y_{\eta_{i\alpha}} D_{N\alpha} Y_{\eta_{\alpha j}}^T}{(4\pi)^2} \left(\frac{m_R^2}{m_R^2 - D_{N\alpha}^2} \ln \left[\frac{m_R^2}{D_{N\alpha}^2} \right] - \frac{m_I^2}{m_I^2 - D_{N\alpha}^2} \ln \left[\frac{m_I^2}{D_{N\alpha}^2} \right] \right), \quad (\text{III.4})$$

where m_I and m_R are, respectively, masses of imaginary and real parts of neutral component in η . Then, the neutrino mass matrix is diagonalized by the PMNS unitary matrix, U_{PMNS} , as $U_{PMNS} m_\nu U_{PMNS}^T = \text{diag}(m_{\nu_1}, m_{\nu_2}, m_{\nu_3}) \equiv D_\nu$, since the charged-lepton mass matrix is diagonal in our model. Note that the constraint for sum of neutrino mass $\text{Tr}[D_\nu] \lesssim 0.12$ eV is given by the data of recent cosmological observations [42]. Each of mixing angle is given in terms of the component of U_{PMNS} as follows:

$$\sin^2 \theta_{13} = |(U_{PMNS})_{13}|^2, \quad \sin^2 \theta_{23} = \frac{|(U_{PMNS})_{23}|^2}{1 - |(U_{PMNS})_{13}|^2}, \quad \sin^2 \theta_{12} = \frac{|(U_{PMNS})_{12}|^2}{1 - |(U_{PMNS})_{13}|^2}. \quad (\text{III.5})$$

In addition, the effective mass for the neutrinoless double beta decay is given by

$$m_{ee} = |D_{\nu_1} \cos^2 \theta_{12} \cos^2 \theta_{13} + D_{\nu_2} \sin^2 \theta_{12} \cos^2 \theta_{13} e^{i\alpha_{21}} + D_{\nu_3} \sin^2 \theta_{13} e^{i(\alpha_{31} - 2\delta_{CP})}|, \quad (\text{III.6})$$

where its observed value could be tested by KamLAND-Zen in future [43].

To carry out numerical analysis, we derive several relations between the normalized neutrino mass matrix and our parameters as follows:

$$\begin{aligned} \tilde{m}_{\nu_{ij}} &\equiv \frac{m_{\nu_{ij}}}{k_3} \approx \frac{1}{(4\pi)^2} \sum_{\alpha=1-3} Y_{\eta_{i\alpha}} \tilde{k}_\alpha Y_{\eta_{\alpha j}}^T, \quad \tilde{k}_\alpha \equiv \frac{k_\alpha}{k_3}, \\ k_\alpha &\equiv D_{N\alpha} \left(\frac{m_R^2}{m_R^2 - D_{N\alpha}^2} \ln \left[\frac{m_R^2}{D_{N\alpha}^2} \right] - \frac{m_I^2}{m_I^2 - D_{N\alpha}^2} \ln \left[\frac{m_I^2}{D_{N\alpha}^2} \right] \right) \\ &\approx D_{N\alpha} \Delta m^2 \left(\frac{D_{N\alpha}^2 - m_R^2 + D_{N\alpha}^2 \ln \left(\frac{m_R^2}{D_{N\alpha}^2} \right)}{(D_{N\alpha}^2 - m_R^2)^2} \right), \end{aligned} \quad (\text{III.7})$$

where the last line is the first order approximation in terms of the small mass difference between m_R^2 and m_I^2 defined by $m_R^2 - m_I^2 = \Delta m^2$.² Then, the normalized neutrino mass eigenvalues are written in terms of neutrino mass eigenvalues; $\text{diag}(\tilde{m}_{\nu_1}^2, \tilde{m}_{\nu_2}^2, \tilde{m}_{\nu_3}^2) = \text{diag}(m_{\nu_1}^2, m_{\nu_2}^2, m_{\nu_3}^2)/k_3^2$. It is then found that k_3^2 is given by

$$k_3^2 = \frac{\Delta m_{\text{atm}}^2}{\tilde{m}_{\nu_3}^2 - \tilde{m}_{\nu_1}^2}, \quad (\text{III.8})$$

² Advantage of this approximation is that \tilde{k}_α does not depend on Δm .

where normal hierarchy is assumed here and Δm_{atm}^2 is the atmospheric neutrino mass difference square. Thus, comparing Eq.(III.7) and Eq.(III.8), we can rewrite Δm^2 by other parameters as follows:

$$\Delta m^2 \approx k_3 \left(\frac{D_{N3} \left[D_{N3}^2 - m_R^2 + D_{N3}^2 \ln \left(\frac{m_R^2}{D_{N3}^2} \right) \right]}{(D_{N3}^2 - m_R^2)^2} \right)^{-1}. \quad (\text{III.9})$$

The solar neutrino mass difference square is also found as

$$\Delta m_{\text{sol}}^2 = \Delta m_{\text{atm}}^2 \frac{\tilde{m}_{\nu_2}^2 - \tilde{m}_{\nu_1}^2}{\tilde{m}_{\nu_3}^2 - \tilde{m}_{\nu_1}^2}, \quad (\text{III.10})$$

In numerical analysis, we require this value to be within the experimental result, while we take Δm_{atm}^2 as an input parameter.

IV. NUMERICAL ANALYSIS

We show numerical analysis to satisfy all of the constraints that we discussed above, where we assume $m_R \approx m_I \approx m_{\eta^\pm}$ to avoid the constraint of oblique parameters. Also, we impose the recent cosmological data; $\text{Tr}[D_\nu] \lesssim 0.12$ eV.³ Then, we provide the experimentally allowed ranges for neutrino mixings and mass difference squares at 3σ range [45] as follows:

$$\begin{aligned} \Delta m_{\text{atm}}^2 &= [2.431 - 2.622] \times 10^{-3} \text{ eV}^2, \quad \Delta m_{\text{sol}}^2 = [6.79 - 8.01] \times 10^{-5} \text{ eV}^2, \\ \sin^2 \theta_{13} &= [0.02044 - 0.02437], \quad \sin^2 \theta_{23} = [0.428 - 0.624], \quad \sin^2 \theta_{12} = [0.275 - 0.350]. \end{aligned} \quad (\text{IV.1})$$

The range of absolute values in three dimensionless parameters $\alpha_\nu, \beta_\nu, \gamma_\nu$ are taken to be [0.1–1], while the mass parameters M_1 is of the order 100 TeV. We also choose $m_R = 534 \pm 8.5$ GeV and $m_I = \sqrt{m_R^2 + \Delta m^2}$ for inert scalar mass.

Fig. 1 shows the sum of neutrino masses $\sum m (\equiv \sum D_\nu)$ versus $\sin^2 \theta_{12}$ (red color) and $\sin^2 \theta_{23}$ (blue color) in the left figure and $\sin^2 \theta_{13}$ (blue color) in the right figure. Here, the horizontal black solid lines are the best fit values, the green dotted lines show 3σ range, and the vertical black line shows upper bound on the cosmological data as shown in the neutrino section. It suggests that all the three mixings run over the experimental ranges, while $\sum m$ is allowed by the narrow range of [0.065–0.070] eV that is always below the cosmological bound 0.12 eV.

³ If this constraint is removed, another allowed range can be found.

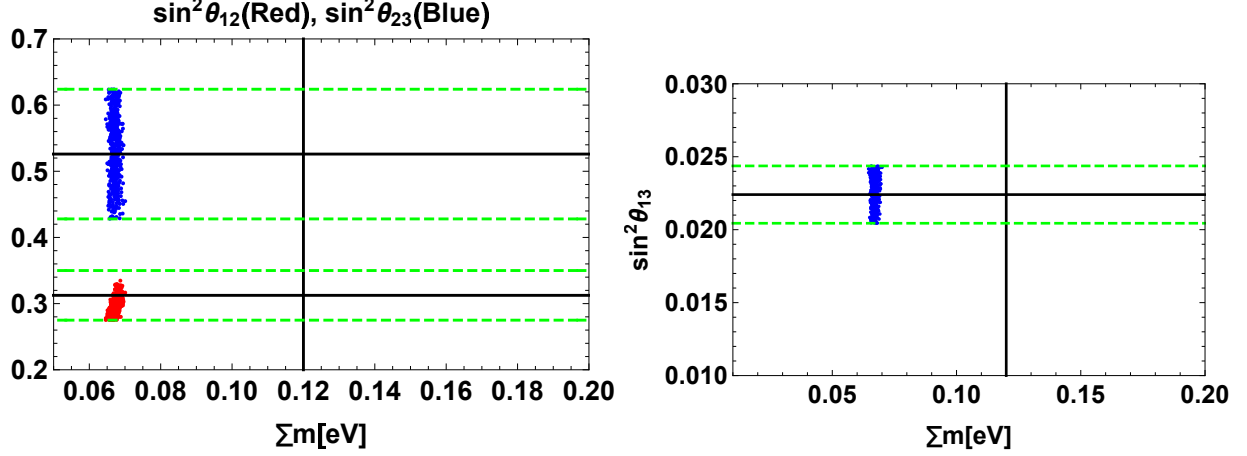


FIG. 1: The sum of neutrino masses $\sum m (\equiv \sum D_\nu)$ versus $\sin^2 \theta_{12}$ (red color) and $\sin^2 \theta_{23}$ (blue color) in the left figure and $\sin^2 \theta_{13}$ (blue color) in the right figure. Here, the horizontal black solid lines are the best fit values, the green dotted lines show 3σ range, and the vertical black line shows upper bound on the cosmological data as shown in the neutrino section.

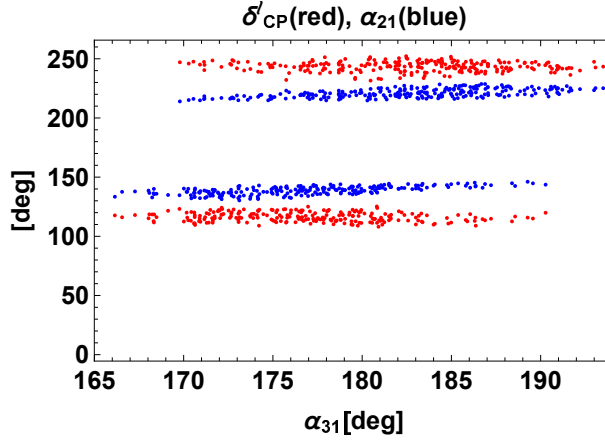


FIG. 2: Phases of δ_{CP}^l (red color) and α_{21} (blue color) in terms of α_{31} .

Fig. 2 shows phases of δ_{CP}^l (red color) and α_{21} (blue color) in terms of α_{31} . This figure implies that Dirac CP is allowed by the range $[100-120, 230-250]$ [deg], α_{21} is $[130-150, 210-230]$ [deg], and α_{31} is $[165-190]$ [deg].

Fig. 3 demonstrates the lightest neutrino mass versus the effective mass for the neutrinoless double beta decay. It suggests that $0.0049 \lesssim m_1 \lesssim 0.0072$ eV and $0.002 \lesssim \langle m_{ee} \rangle \lesssim 0.005$ eV. Another remarks are in order:

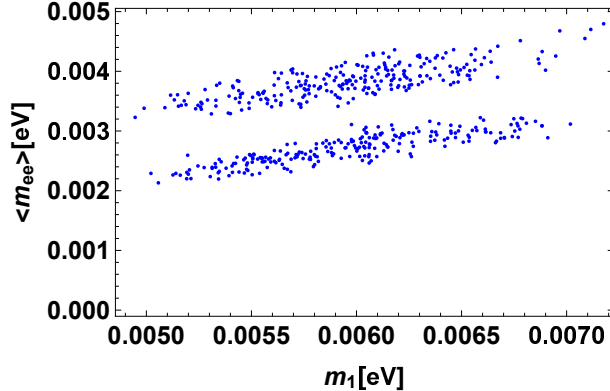


FIG. 3: The lightest neutrino mass versus the effective mass for the neutrinoless double beta decay.

1. The typical region of modulus τ is found in rather narrow modular field space as $0.43 \lesssim \text{Re}[\tau] \lesssim 0.45$ and $0.65 \lesssim \text{Im}[\tau] \lesssim 0.67$.
2. The Majorana mass eigenvalues are in the range of

$$D_{N_1} = [40 - 230] \text{ TeV}, \quad D_{N_2} = [80 - 520] \text{ TeV}, \quad D_{N_3} = [100 - 750] \text{ TeV}.$$

We also show correlation among the mass eigenvalues in Fig. 4. Note that the mass scale is larger than the previous model in ref. [6] which is due to simpler loop structure requiring heavier masses of N_i .

3. Typical scale of cLFVs tends to be very small in our analyses as shown in Fig. 5, therefore following upper bounds are realized:

$$\text{BR}(\mu \rightarrow e\gamma) \lesssim 6.0 \times 10^{-15}, \quad \text{BR}(\tau \rightarrow e\gamma) \lesssim 1.2 \times 10^{-15}, \quad \text{BR}(\tau \rightarrow \mu\gamma) \lesssim 1.7 \times 10^{-14}.$$

These values are smaller than the models in ref. [6, 11] which is due to heavier mass scale of N_i .

Note that DM candidate in our scenario is inert scalar η_R since N_1 is much heavier. The mass value of $m_R \sim 530$ GeV can accommodate with observed relic density of DM via gauge interaction taking into account coannihilation processes [46]. We also need to assume small Higgs portal coupling to avoid DM direct detection constraints. In principle, our DM phenomenology is the same as of the canonical inert Higgs doublet model and we do not discuss it in this paper.

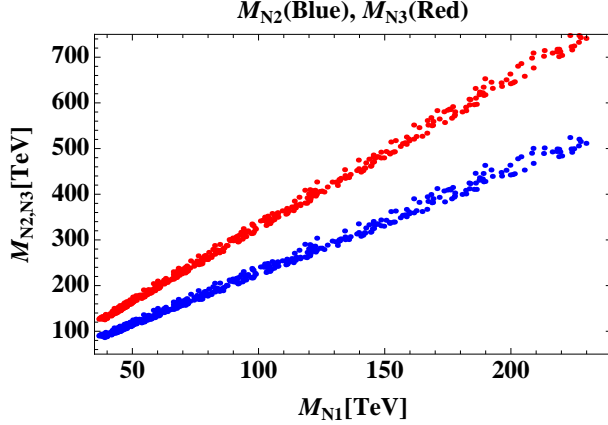


FIG. 4: The correlations among masses of N_i where red(blue) color points correspond to $M_{N_1} - M_{N_{3(2)}}$ correlation.

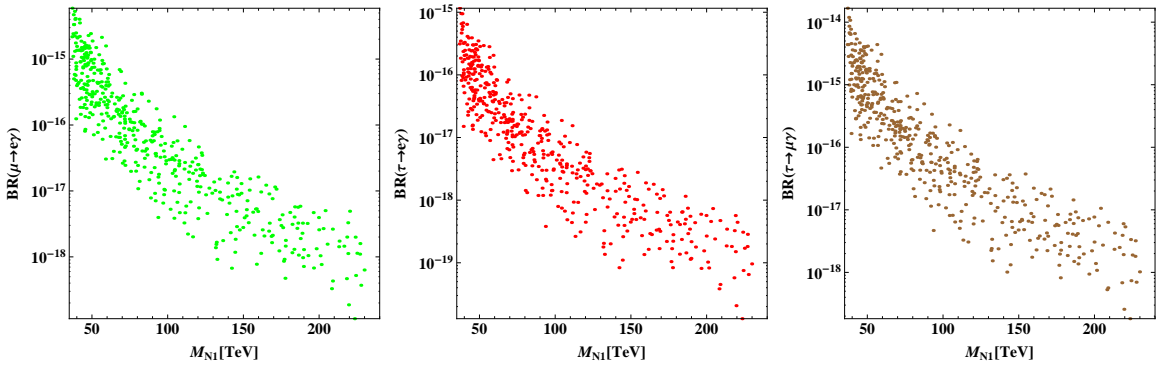


FIG. 5: The BRs for cLFV processes $\ell \rightarrow \ell' \gamma$ as functions of the mass of N_1 .

V. CONCLUSION AND DISCUSSION

We have studied a model based on modular A_4 symmetry in which neutrino masses are generated radiatively at one-loop level. The minimal Scotogenic scenario can be realized using modular form with higher weight where we have much simpler field contents compared to previous modular A_4 radiative neutrino mass generation model with the modular form of lowest weight given in ref. [6]. The modular A_4 symmetry plays a role of restricting interactions, generating neutrino mass and stabilizing DM candidate. We have formulated lepton flavor violation and neutrino mass matrix in the model. Then numerical analysis has been carried out to find prediction of our scenario. In our numerical analyses, we have highlightend several remarks as follows:

1. Three mixings cover all the experimental results by 3σ interval, but the sum of neutrino masses are the narrow range $[0.065, 0.0070]$ eV that is below the upper bound of cosmological data of 0.12 eV.
2. Dirac CP is allowed by the range $[100-120, 230-250]$ [deg], α_{21} is $[130-150, 210-230]$ [deg], and α_{31} is $[165-190]$ [deg].
3. We found the following regions; $0.0049 \lesssim m_1 \lesssim 0.0072$ eV and $0.002 \lesssim \langle m_{ee} \rangle \lesssim 0.005$ eV which can be seen from Fig. 3.

These predictions will be tested in the near future. In fact, comparing with previous one-loop models with modular A_4 in ref. [6, 11], we find prediction for CP-phases are different although that for neutrino mass and mixing are similar. Thus it would be possible to distinguish these models by measuring CP-phase such as Dirac phase δ_{CP}^l in future experiments. The DM candidate in our scenario is inert scalar boson and its mass is chosen to be ~ 530 GeV. DM phenomenology is the same as of the canonical inert Higgs doublet model and our DM mass value can accommodate the observed relic density of DM via gauge interaction taking into account coannihilation processes. We also require small Higgs portal coupling to avoid DM direct detection constraints, which can be easily realized by choosing parameters in the potential.

Acknowledgments

This research was supported by an appointment to the JRG Program at the APCTP through the Science and Technology Promotion Fund and Lottery Fund of the Korean Government. This was also supported by the Korean Local Governments - Gyeongsangbuk-do Province and Pohang City (H.O.). H. O. is sincerely grateful for the KIAS member, and log cabin at POSTECH to provide nice space to come up with this project. OP is supported by the National Research Foundation of Korea Grants No. 2017K1A3A7A09016430 and No.

- [1] R. de Adelhart Toorop, F. Feruglio and C. Hagedorn, Nucl. Phys. B **858**, 437 (2012) [arXiv:1112.1340 [hep-ph]].
- [2] F. Feruglio, doi:10.1142/9789813238053_0012 arXiv:1706.08749 [hep-ph].
- [3] J. C. Criado and F. Feruglio, arXiv:1807.01125 [hep-ph].
- [4] T. Kobayashi, N. Omoto, Y. Shimizu, K. Takagi, M. Tanimoto and T. H. Tatsuishi, JHEP **1811**, 196 (2018) doi:10.1007/JHEP11(2018)196 [arXiv:1808.03012 [hep-ph]].
- [5] H. Okada and M. Tanimoto, Phys. Lett. B **791**, 54 (2019) doi:10.1016/j.physletb.2019.02.028 [arXiv:1812.09677 [hep-ph]].
- [6] T. Nomura and H. Okada, arXiv:1904.03937 [hep-ph].
- [7] H. Okada and M. Tanimoto, arXiv:1905.13421 [hep-ph].
- [8] F. J. de Anda, S. F. King and E. Perdomo, arXiv:1812.05620 [hep-ph].
- [9] P. P. Novichkov, S. T. Petcov and M. Tanimoto, arXiv:1812.11289 [hep-ph].
- [10] T. Nomura and H. Okada, arXiv:1906.03927 [hep-ph].
- [11] H. Okada and Y. Orikasa, arXiv:1907.13520 [hep-ph].
- [12] T. Kobayashi, K. Tanaka and T. H. Tatsuishi, Phys. Rev. D **98** (2018) no.1, 016004 [arXiv:1803.10391 [hep-ph]].
- [13] T. Kobayashi, Y. Shimizu, K. Takagi, M. Tanimoto, T. H. Tatsuishi and H. Uchida, Phys. Lett. B **794**, 114 (2019) doi:10.1016/j.physletb.2019.05.034 [arXiv:1812.11072 [hep-ph]].
- [14] T. Kobayashi, Y. Shimizu, K. Takagi, M. Tanimoto and T. H. Tatsuishi, arXiv:1906.10341 [hep-ph].
- [15] H. Okada and Y. Orikasa, arXiv:1907.04716 [hep-ph].
- [16] J. T. Penedo and S. T. Petcov, Nucl. Phys. B **939**, 292 (2019) doi:10.1016/j.nuclphysb.2018.12.016 [arXiv:1806.11040 [hep-ph]].
- [17] P. P. Novichkov, J. T. Penedo, S. T. Petcov and A. V. Titov, JHEP **1904**, 005 (2019) doi:10.1007/JHEP04(2019)005 [arXiv:1811.04933 [hep-ph]].
- [18] T. Kobayashi, Y. Shimizu, K. Takagi, M. Tanimoto and T. H. Tatsuishi, arXiv:1907.09141 [hep-ph].
- [19] P. P. Novichkov, J. T. Penedo, S. T. Petcov and A. V. Titov, arXiv:1812.02158 [hep-ph].

- [20] G. J. Ding, S. F. King and X. G. Liu, arXiv:1903.12588 [hep-ph].
- [21] A. Baur, H. P. Nilles, A. Trautner and P. K. S. Vaudrevange, arXiv:1901.03251 [hep-th].
- [22] I. de Medeiros Varzielas, S. F. King and Y. L. Zhou, arXiv:1906.02208 [hep-ph].
citeLiu:2019khw
- [23] X. G. Liu and G. J. Ding, arXiv:1907.01488 [hep-ph].
- [24] G. Altarelli and F. Feruglio, Rev. Mod. Phys. **82** (2010) 2701 [arXiv:1002.0211 [hep-ph]].
- [25] H. Ishimori, T. Kobayashi, H. Ohki, Y. Shimizu, H. Okada and M. Tanimoto, Prog. Theor. Phys. Suppl. **183** (2010) 1 [arXiv:1003.3552 [hep-th]].
- [26] H. Ishimori, T. Kobayashi, H. Ohki, H. Okada, Y. Shimizu and M. Tanimoto, Lect. Notes Phys. **858** (2012) 1, Springer.
- [27] D. Hernandez and A. Y. Smirnov, Phys. Rev. D **86** (2012) 053014 [arXiv:1204.0445 [hep-ph]].
- [28] S. F. King and C. Luhn, Rept. Prog. Phys. **76** (2013) 056201 [arXiv:1301.1340 [hep-ph]].
- [29] S. F. King, A. Merle, S. Morisi, Y. Shimizu and M. Tanimoto, arXiv:1402.4271 [hep-ph].
- [30] S. F. King, Prog. Part. Nucl. Phys. **94** (2017) 217 doi:10.1016/j.pnpnp.2017.01.003 [arXiv:1701.04413 [hep-ph]].
- [31] S. T. Petcov, Eur. Phys. J. C **78** (2018) no.9, 709 [arXiv:1711.10806 [hep-ph]].
- [32] A. Baur, H. P. Nilles, A. Trautner and P. K. S. Vaudrevange, arXiv:1908.00805 [hep-th].
- [33] E. Ma, Phys. Rev. D **73**, 077301 (2006) doi:10.1103/PhysRevD.73.077301 [hep-ph/0601225].
- [34] M. Hirsch, S. Morisi, E. Peinado and J. W. F. Valle, Phys. Rev. D **82**, 116003 (2010) doi:10.1103/PhysRevD.82.116003 [arXiv:1007.0871 [hep-ph]].
- [35] J. M. Lamprea and E. Peinado, Phys. Rev. D **94**, no. 5, 055007 (2016) doi:10.1103/PhysRevD.94.055007 [arXiv:1603.02190 [hep-ph]].
- [36] L. M. G. De La Vega, R. Ferro-Hernandez and E. Peinado, Phys. Rev. D **99**, no. 5, 055044 (2019) doi:10.1103/PhysRevD.99.055044 [arXiv:1811.10619 [hep-ph]].
- [37] P. P. Novichkov, J. T. Penedo, S. T. Petcov and A. V. Titov, arXiv:1905.11970 [hep-ph].
- [38] S. Baek, T. Nomura and H. Okada, Phys. Lett. B **759**, 91 (2016) doi:10.1016/j.physletb.2016.05.055 [arXiv:1604.03738 [hep-ph]].
- [39] A. M. Baldini *et al.* [MEG Collaboration], Eur. Phys. J. C **76**, no. 8, 434 (2016) [arXiv:1605.05081 [hep-ex]].
- [40] F. Renga [MEG Collaboration], Hyperfine Interact. **239**, no. 1, 58 (2018) [arXiv:1811.05921 [hep-ex]].

- [41] B. Aubert *et al.* [BaBar Collaboration], Phys. Rev. Lett. **104** (2010) 021802 [arXiv:0908.2381 [hep-ex]].
- [42] N. Aghanim *et al.* [Planck Collaboration], arXiv:1807.06209 [astro-ph.CO].
- [43] A. Gando *et al.* [KamLAND-Zen Collaboration], Phys. Rev. Lett. **117**, no. 8, 082503 (2016) Addendum: [Phys. Rev. Lett. **117**, no. 10, 109903 (2016)] doi:10.1103/PhysRevLett.117.109903, 10.1103/PhysRevLett.117.082503 [arXiv:1605.02889 [hep-ex]].
- [44] T. Hambye, F.-S. Ling, L. Lopez Honorez and J. Rocher, JHEP **0907**, 090 (2009) Erratum: [JHEP **1005**, 066 (2010)] doi:10.1007/JHEP05(2010)066, 10.1088/1126-6708/2009/07/090 [arXiv:0903.4010 [hep-ph]].
- [45] I. Esteban, M. C. Gonzalez-Garcia, A. Hernandez-Cabezudo, M. Maltoni and T. Schwetz, JHEP **1901**, 106 (2019) doi:10.1007/JHEP01(2019)106 [arXiv:1811.05487 [hep-ph]].
- [46] A. Arhrib, Y. L. S. Tsai, Q. Yuan and T. C. Yuan, JCAP **1406**, 030 (2014) doi:10.1088/1475-7516/2014/06/030 [arXiv:1310.0358 [hep-ph]].